Rotational Spectroscopy of a Triatomic Molecular Anion

Olga Lakhmanskaya,[1] Malcolm Simpson,[1] Simon Murauer,[1] Markus Nötzold,[1]
Eric Endres,[1,*] Viatcheslav Kokoouline,[1,2] and Roland Wester[1,†]
[1]*Institut für Ionenphysik und Angewandte Physik, Universität Innsbruck, Technikerstraße 25, 6020 Innsbruck, Austria*
[2]*Department of Physics, University of Central Florida,*
4111 Libra Drive, Physical Sciences Building 430, Orlando, Florida 32816-2385, USA

(Received 1 March 2018; published 22 June 2018)

Rotational transitions of the nonlinear triatomic molecular anion NH_2^- have been observed by terahertz spectroscopy in a cryogenic radio frequency ion trap. Absorption of terahertz photons has been probed by rotational state-dependent photodetachment of the trapped negative ions near the detachment threshold. Using this two-photon scheme, the two lowest rotational transitions for the asymmetric top rotor NH_2^- have been found. For the para nuclear spin configuration, the $1_0 \leftarrow 0_0$ transition frequency was determined to be 933 954(2) MHz, and for the ortho configuration the $1_{+1} \leftarrow 1_{-1}$ transition frequency was determined to be 447 375(3) MHz. This result appears to preclude the recent tentative assignment of an interstellar absorption feature to NH_2^-.

DOI: 10.1103/PhysRevLett.120.253003

Molecular ions in traps are extensively studied to improve the limits in precision spectroscopy, to unravel the properties of chemically and biologically important species, and to provide benchmark data for comparison with astronomical observations. In radio frequency quadrupole trap sympathetic cooling, a high level of control and long interrogation times have been used to study forbidden and overtone vibrational transitions in diatomic molecular cations [1–3]. Nondestructive detection of an electronic transition has been achieved with quantum logic spectroscopy [4]. In radio frequency multipole traps and in electrostatic storage rings, a range of organic and biological molecules have been studied, such as nonrigid protonated methane [5], protonated amino acids [6], and biochromophores [7]. Also, many molecular ions that are important in interstellar molecular clouds have been studied in multipole ion traps [8–10]. In all cases, the ability to control the molecular rotational and vibrational quantum states by neutral buffer gas is important [11,12].

Interstellar negative ions and their role in astrochemical networks have been debated since the 1970s [13,14], but it was not until 2006 that the first interstellar molecular anion was detected [15]. Since then, six different carbon-containing molecular anions have been discovered in several different interstellar and circumstellar clouds [16,17]. The combination of radioastronomical observation, laboratory spectroscopy, and theoretical modeling has proven crucial for these discoveries. The observed abundances still hold many open questions. Many years ago it was suggested that radiative electron attachment to a neutral molecule is the most important mechanism for anion formation in space [14]. However, for some of the anions, notably the smallest one CN^-, this mechanism was found not to proceed at a sufficient rate [18]. To form this, and possibly other negative ions, the reaction with atomic hydrogen anions H^- is suggested [18,19], and indirect means to detect this anion have been proposed [20].

Recently, NH_2^-, a molecular anion with a similarly small electron binding energy as H^-, has been tentatively assigned to a previously unidentified absorption feature near 934 GHz [21]. However, astrochemical model calculations by the same authors predict an expected abundance of NH_2^- far below the detection limit. NH_2^- is a closed shell asymmetric top rotor, analogous to the neutral water molecule. The only available A, B, and C rotational constants have been determined by rotationally resolved vibrational spectroscopy [22]. Those measurements predict the fundamental rotational transition at 934.0 GHz with a significant uncertainty of about 230 MHz (see Table I below), which does not exclude the tentative detection. More recent *ab initio* electronic structure calculations gave a lower value by about 1.4 GHz [23]. Consequently, direct rotational spectra of NH_2^- are required to test the assignment and the theoretical calculations and to facilitate new astronomical searches.

To detect rotational transitions in trapped molecular ions, indirect schemes are required due to the small number densities in radio frequency traps. The first such measurements date from 2008 [24]. The lowest lying transitions of para-H_2D^+ and ortho-D_2H^+ have been detected by applying the laser induced reaction technique (LIR) [25]. Another scheme is infrared (sub)-mm double resonance LIR, which was applied to CH_2D^+ [26], CD_2H^+ [27], and OH^- [28]. Rotational state-dependent attachment of He atoms to cold molecules has been successfully applied to CD^+ [29], l-C_3H^+ [9], CF^+, and NH_3D^+ [30]. Terahertz-visible

TABLE I. Comparison of frequencies (in MHz) of the rotational transitions for NH_2^- measured or derived in this Letter and in previous studies.

$J' \leftarrow J$	This Letter	Astronomy Ref. [21]	Experiment Ref. [22]	Theory Ref. [23]
$1_0 \leftarrow 0_0$	933 954.2(0.1)(2)[a]	933 973–934 009	934 003(233)	932 624.5[b]
$1_1 \leftarrow 1_{-1}$	447 375.1(0.3)(3)[a]	⋯	447 208(233)	445 897.3[b]

[a]Observed in experiment: the first bracket denotes statistical error, and the second one shows systematic uncertainty caused by the wave meter.
[b]Transition frequencies have been derived based on spectroscopic constants in Table VII (column: $+rel+3-ptAC/AVXZ$).

two-photon rotational spectroscopy is an alternative method that has been developed in our group to probe rotational transitions of molecular anions, and this has been applied to OD^- [31].

Here we present rotational absorption measurements for the lowest two rotational transitions in the triatomic molecular anion NH_2^-. The rotational energy level diagrams of this ion and its corresponding neutral are presented in Fig. 1. Both molecules belong to the C_{2v} symmetry group, and their ground electronic states are $X\,^1A_1$ for NH_2^- and $X\,^2B_1$ for NH_2. Rotational levels are identified with N_K ($K = K_a - K_c$), where N is the rotational angular momentum quantum number and K_a and K_c are the projection quantum numbers of the prolate and oblate rotors, with which the asymmetric top rotational levels correlate. Given the symmetry of the rotational states of NH_2^-, the selection rules $\Delta J = 0, \pm 1, \Delta K_a = \pm 1, \pm 3, \ldots, \Delta K_c = \pm 1, \pm 3, \ldots$ apply for rotational transitions [32]. Because of the presence of equivalent hydrogen nuclei, one distinguishes ortho and para states, which cannot be connected by rotational transitions. For NH_2^-, para states are characterized by even K values and ortho rotational levels are characterized by odd K. For neutral NH_2, the symmetries of the ortho- and para rotational states are inverted. The energy levels in Fig. 1 are calculated with the spectroscopic constants obtained in previous studies [22,33]. The fine and hyperfine energy splittings are omitted. The fine structure splitting of NH_2 is about 4–16 GHz, and hyperfine levels are separated by a few tens of MHz [33,34]. In the case of NH_2^-, only hyperfine splittings may occur, but no splitting constants are known. The lowest rotational transitions in para- and ortho-NH_2^- are shown in Fig. 1 as thick arrows; photodetachment transitions to neutral NH_2 are plotted as thin arrows.

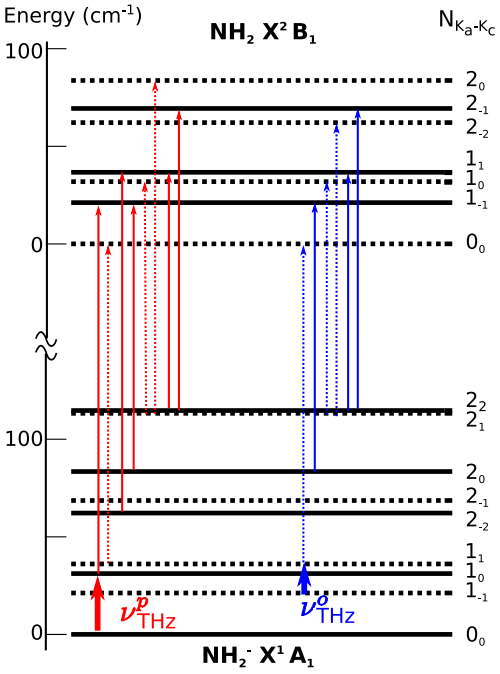

FIG. 1. NH_2^- and NH_2 rotational energy-level diagram showing the allowed PD transitions for the s-wave electron (A_1 symmetry) and rotational excitations detected in THz spectroscopy. The levels and transitions corresponding to ortho states are indicated with dashed lines and arrows. The red and blue colors are used to distinguish transitions involved in the spectroscopy of para-NH_2^- and ortho-NH_2^-, respectively.

The experiment has been carried out in our 22-pole radio frequency ion trap setup [8]. NH_2^- ions are produced in a pulsed jet of the gas mixture $He - NH_3$ (90%, 10%) in a plasma discharge and loaded into the 22-pole ion trap [35,36]. Multiple ion pulses are loaded within a few hundred milliseconds, which improves the stability of the trapped ion intensity. During the experiment, the trap—together with its thermal shield—is cooled to 9(1) K. He buffer gas with a density of $1.8 - 2.5 \times 10^{10}$ cm^{-3} thermalizes with the trap shield and collisionally cools the ions both internally and translationally. On top of the He buffer gas level, some additional gas flows from the source chamber to the trap. Its partial pressure outside the trap is about $(1-4) \times 10^{-8}$ mbar leading to a neutral density contribution inside the trap below 3×10^9 cm^{-3}. It is known from previous studies that the internal and translational ion temperatures do not follow exactly the trap temperature [24,28,37,38], the reasons for which are not completely understood [39]. However, it is safe to assume that the internal ion temperature lies between 10 and 30 K.

The cw THz radiation used to drive rotational transitions is generated by difference frequency mixing of two distributed feedback (DFB) diode lasers on a commercially available photomixer (TOPTICA) over a continuous range from 0.1 to 1.6 THz with powers ranging between about

1.2 μW (at 0.1 THz) and about 20 nW (at 1.6 THz). The radiation is continuously transmitted into the trap. In the current geometry, the transfer efficiency is less than 10% due to scattering and diffraction of the radiation with 0.2–3 mm wavelength at the 6.6 mm trap opening [31]. The THz frequency is continuously monitored with a high-resolution wave meter (HighFinesse WS-U). The linewidth of the radiation and the absolute calibration of the wave meter were determined by observing several rotational transitions of carbon monoxide and acetonitrile in a gas cell. The calibration measurements, performed on different days, showed fluctuating wave meter frequency offsets ranging from -1.2 ± 0.7 MHz to 2.4 ± 1.3 MHz. Based on this, an overall systematic accuracy of 2 MHz is assigned to the frequency calibration. This estimate can be improved in the future by recording the calibration in parallel to the measurements. Since the CO lines are known to have very low pressure broadening coefficients (3 MHz/mbar [40]), they were also used to determine the linewidth of the THz radiation. According to Lorentzian fits, the FWHM ranges between 2 and 5 MHz, depending on the temperature and current settings of the DFB lasers used to generate the THz radiation.

To probe the rotational excitation, a self-built tunable external cavity laser near 1600 nm is added for near-threshold photodetachment of NH_2^-. This grating-stabilized laser in the Littrow configuration is based on a single angled facet gain chip, and it shows a tuning range of about $6000 - 6750$ cm^{-1}. THz radiation and photodetachment laser beam counterpropagate along the trap axis and enter the trap through end-cap electrodes. The photodetachment laser with power of about 5–6 mW is admitted only after 6 s of trapping time to ensure complete thermalization and is turned off 100 ms before the ions are extracted. The detachment laser is fixed at 6245 and 6215 cm^{-1} for the ortho- and para-NH_2^- transitions, respectively. The choice of the photodetachment laser frequency assures that only the states with $N_K \geq 1_0$ for para-NH_2^- and with $N_K \geq 1_1$ for ortho-NH_2^- are involved in photodetachment transitions. These frequencies are selected by performing scans below the photodetachment threshold for different buffer gas temperatures. In this way, we have identified ranges in which the detachment rate depends on the thermal rotational excitation of the trapped ions. This is caused by photodetachment from rotationally excited states in the anion, as found previously for OH^- [31,37]. The results of these measurements are described in detail in Ref. [41].

For the rotational spectroscopy measurements, the frequency of the THz source is scanned over a range in which an allowed rotational transition is expected. The photodetachment frequency is fixed during these scans. Off resonance, the detachment leads to an exponential decay of the trapped ion intensity with photodetachment rates of about 0.2 s^{-1} in the case of spectroscopy of para-NH_2^- and 0.07 s^{-1} in the case of ortho-NH_2^-. This rate is always measured before starting terahertz spectroscopy scans. When the THz radiation is on resonance with a rotational transition, it establishes a higher population in the respective upper rotational state. This rotational excitation increases the photodetachment rate and can be observed as a drop in the ion intensity. The residual ion intensity after an exposure time of 13 s (para-NH_2^-) and 30 s (ortho-NH_2^-) is detected by extracting the ions from the trap and passing them onto a charge-integrating microchannel plate detector. To reach a higher sensitivity compared to our previous experiment with OD^- [31], the buffer gas density is reduced by a factor of 20. Thus, inelastic relaxation collisions with helium buffer gas atoms, which counteract the THz excitation, happen at a lower rate. The photodetachment exposure time has been chosen to be between two and three inverse decay rates, which has proven in simulations to yield the highest sensitivity to terahertz excitation.

The line search was performed around 934 and 447.5 GHz for almost 1 GHz, and absorption was found near 933.95 and 447.38 GHz. Figure 2 shows two measured spectra with the two transitions in para-NH_2^- and ortho-NH_2^-. To obtain these spectra, the individual frequency points have been sorted into a series of frequency intervals (bins). Each bin has a width of 1.8 MHz (for para-NH_2^-) or 1.6 MHz (for ortho-NH_2^-). They contain the average of 2–12 of the original measurement points. The error bars attributed to the ion intensities are obtained from the rms deviations of these points. To fit the observed absorption profiles, a first-order polynomial is fitted to the ion intensity outside the line profile to determine the background rate and to account for possible small linear drifts. Then the measured lines are fitted to a sum of the fixed background function and a Lorentzian profile with three free parameters. For the data presented in Fig. 2, the obtained center frequencies and their statistical accuracies are $933\,953.3 \pm 1.0$ MHz and $447\,376.5 \pm 0.3$ MHz, respectively.

In this way, we have collected 23 independent measurements of the para-NH_2^- absorption frequencies. Combining these data and taking into account the mean wave meter offset of 0.76 ± 0.03 MHz, we obtain the rotational transition of para-NH_2^- $0_0 \rightarrow 1_0$ of 933 954.2(0.1)(2) MHz. The first error bar is the statistical accuracy of the weighted average; the second one arises from the wave meter calibration as discussed above. We identify the line for ortho-NH_2^- with a larger systematic uncertainty of ± 3 MHz because we had less information about the wave meter drifts at this line position. The frequency for transition $1_{-1} \rightarrow 1_1$ is found to be 447 375.1(0.3)(3) MHz, showing again both statistical and systematic accuracy. The average linewidth of the two observed transitions is 6.4(5) MHz (FWHM). This is slightly larger than the linewidth of the THz radiation described above. The Doppler broadening (FWHM) below 30 K does not exceed 1 MHz for both transitions and therefore cannot explain the

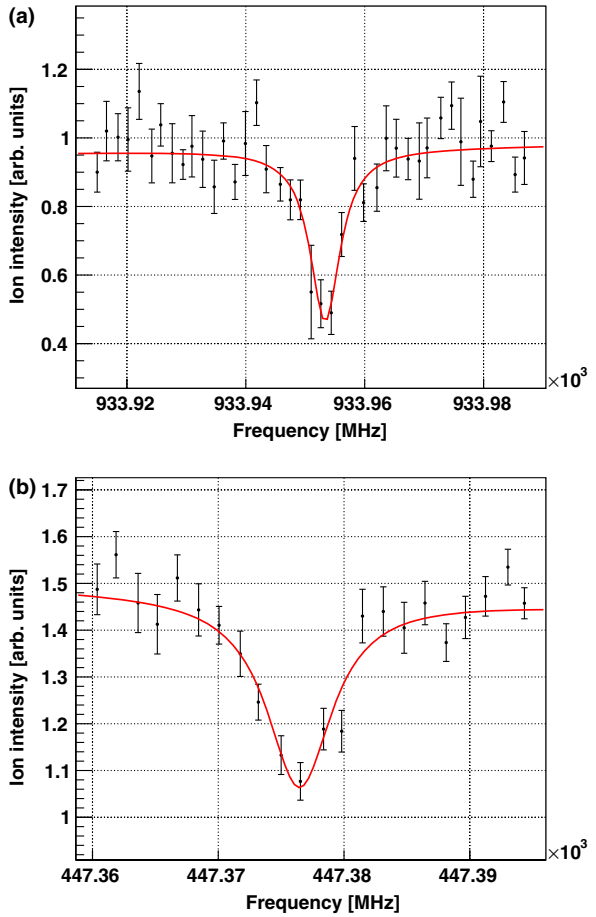

FIG. 2. Histograms of the ion intensity of NH_2^- after photodetachment as a function of the THz radiation frequency. Individual frequency points are combined in bins with a 1.8 MHz (para) or 1.6 MHz (ortho) width. The resonances are observed at $933\,953.3 \pm 1.0$ MHz for para-NH_2^-: $0_0 \rightarrow 1_0$ [panel (a)] and at $447\,376.5 \pm 0.3$ for ortho-NH_2^-: $1_{-1} \rightarrow 1_1$ [panel (b)]. The fitted linewidths of the two transitions are 6.1(5) MHz for para- and 6.4(7) MHz for ortho-NH_2^- (FWHM).

widths. We assume that unresolved line splitting due to rotation-hyperfine coupling may be the cause.

Table I shows the comparison of our line positions with previous results. Our work improves the accuracy of the purely rotational transitions in NH_2^- by 2 orders of magnitude. The only previous experimental study of the amide ion with rotational resolution was performed in the near-infrared [22]. In that work an accuracy for the prediction of the pure rotational transitions of about 200 MHz was achieved. Recently a high-level *ab initio* calculation has been performed to predict purely rotational transitions to aid astronomical observations [23]. For the para transition, our measured line position deviates only by 1.3 GHz from the calculation, which is clear evidence for the quality reached in the *ab initio* calculation.

With our improved line positions, we can test the tentative assignment of an observed transition towards the middle part of the giant molecular cloud Sagittarius B2 [SgrB2(M)] to the NH_2^- anion by Persson *et al.* [21]. Their observation with the Heterodyne Instrument for the Far-Infrared on board the *Herschel Space Observatory* was attributed to a transition with a rest frequency of between 933 973 and 934 009 GHz. The frequency determined in the present study appears to preclude an assignment of the astronomical feature discussed above with para-NH_2^-. While the modeled abundance of this anion is low [21], it is interesting to examine alternative formation pathways. Formation by radiative electron attachment of electrons to NH_2 and also by dissociative electron attachment to ammonia, with an energy threshold of 3.857 eV, was considered, but found inefficient. If NH_2^- is observed, the reaction $H^- + NH_3 \rightarrow NH_2^- + H_2$ may be an important formation mechanism, even though it is slightly endoergic by about 0.14 eV [42]. This reaction would be a tracer for interstellar H^-. These open questions will require further work on astrochemical modeling and towards astronomical searches for the ortho-NH_2^- transition presented here.

Terahertz spectroscopy of cold molecular ions in radio frequency traps has become an important research field for the investigation of molecular properties with high resolution and its comparison with astronomical observations. In the future, further applications to polyatomic ions will allow us to shed more light on molecular structures, in particular for nonrigid molecular systems, on vibration-rotation-tunneling splittings, and on possible other interstellar or planetary ions.

We thank Friedrich Wyrowski and Karl M. Menten for fruitful discussions. This work has been supported by the European Research Council (ERC) under ERC Grant Agreement No. 279898, by the Austrian Science Fund (FWF) through Project No. P29558-N36, and through the Doctoral Programme Atoms, Light, and Molecules, Project No. W1259-N27. V. K. acknowledges support from the National Science Foundation under Grant No. PHY-15-06391 and the Austrian-American Educational Commission.

*Present address: Physikalisches Institut, Universität Heidelberg, Im Neuenheimer Feld 226, 69120 Heidelberg, Germany.
†roland.wester@uibk.ac.at

[1] U. Bressel, A. Borodin, J. Shen, M. Hansen, I. Ernsting, and S. Schiller, Phys. Rev. Lett. **108**, 183003 (2012).
[2] M. Germann, X. Tong, and S. Willitsch, Nat. Phys. **10**, 820 (2014).
[3] J. Biesheuvel, J.-P. Karr, L. Hilico, K. Eikema, W. Ubachs, and J. Koelemeij, Nat. Commun. **7**, 10385 (2016).
[4] F. Wolf, Y. Wan, J. C. Heip, F. Gebert, C. Shi, and P. O. Schmidt, Nature **530**, 457 (2016).
[5] O. Asvany, K. M. T. Yamada, S. Brünken, A. Potapov, and S. Schlemmer, Science **347**, 1346 (2015).

[6] O. V. Boyarkin, S. R. Mercier, A. Kamariotis, and T. R. Rizzo, J. Am. Chem. Soc. **128**, 2816 (2006).
[7] H. V. Kiefer, H. B. Pedersen, A. V. Bochenkova, and L. H. Andersen, Phys. Rev. Lett. **117**, 243004 (2016).
[8] T. Best, R. Otto, S. Trippel, P. Hlavenka, A. von Zastrow, S. Eisenbach, S. Jézouin, R. Wester, E. Vigren, M. Hamberg, and W. D. Geppert, Astrophys. J. **742**, 63 (2011).
[9] S. Brünken, L. Kluge, A. Stoffels, O. Asvany, and S. Schlemmer, Astrophys. J. Lett. **783**, L4 (2014).
[10] S. Brünken, O. Sipilä, E. T. Chambers, J. Harju, P. Caselli, O. Asvany, C. E. Honingh, T. Kamiński, K. M. Menten, J. Stutzki *et al.*, Nature **516**, 219 (2014).
[11] A. K. Hansen, O. O. Versolato, Ł. Kłosowski, S. B. Kristensen, A. Gingell, M. Schwarz, A. Windberger, J. Ullrich, J. R. Crespo López-Urrutia, and M. Drewsen, Nature **508**, 76 (2014).
[12] D. Hauser, S. Lee, F. Carelli, S. Spieler, O. Lakhmanskaya, E. S. Endres, S. S. Kumar, F. Gianturco, and R. Wester, Nat. Phys. **11**, 467 (2015).
[13] A. Dalgarno and R. A. McCray, Astrophys. J. **181**, 95 (1973).
[14] E. Herbst, Nature **289**, 656 (1981).
[15] M. C. McCarthy, C. A. Gottlieb, H. Gupta, and P. Thaddeus, Astrophys. J. Lett. **652**, L141 (2006).
[16] M. Larsson, W. D. Geppert, and G. Nyman, Rep. Prog. Phys. **75**, 066901 (2012).
[17] T. J. Millar, C. Walsh, and T. A. Field, Chem. Rev. **117**, 1765 (2017).
[18] M. Khamesian, N. Douguet, S. F.. dos Santos, O. Dulieu, M. Raoult, W. J. Brigg, and V. Kokoouline, Phys. Rev. Lett. **117**, 123001 (2016).
[19] M. Satta, F. A. Gianturco, F. Carelli, and R. Wester, Astrophys. J. **799**, 228 (2015).
[20] M. Ayouz, R. Lopes, M. Raoult, O. Dulieu, and V. Kokoouline, Phys. Rev. A **83**, 052712 (2011).
[21] C. M. Persson, M. Hajigholi, G. E. Hassel, A. O. H. Olofsson, J. H. Black, E. Herbst, H. S. P. Müller, J. Cernicharo, E. S. Wirström, M. Olberg, Å. Hjalmarson, D. C. Lis, H. M. Cuppen, M. Gerin, and K. M. Menten, Astron. Astrophys. **567**, A130 (2014).
[22] L. M. Tack, N. H. Rosenbaum, J. C. Owrutsky, and R. J. Saykally, J. Chem. Phys. **84**, 7056 (1986).
[23] X. Huang and T. J. Lee, J. Chem. Phys. **131**, 104301 (2009).
[24] O. Asvany, O. Ricken, H. S. P. Müller, M. C. Wiedner, T. F. Giesen, and S. Schlemmer, Phys. Rev. Lett. **100**, 233004 (2008).
[25] S. Schlemmer, E. Lescop, J. von Richthofen, D. Gerlich, and M. A. Smith, J. Chem. Phys. **117**, 2068 (2002).
[26] M. Töpfer, P. Jusko, S. Schlemmer, and O. Asvany, Astron. Astrophys. **593**, L11 (2016).
[27] P. Jusko, A. Stoffels, S. Thorwirth, S. Brünken, and O. Asvany, J. Mol. Spectrosc. **332**, 59 (2017).
[28] P. Jusko, O. Asvany, A.-C. Wallerstein, S. Brünken, and S. Schlemmer, Phys. Rev. Lett. **112**, 253005 (2014).
[29] S. Brünken, L. Kluge, A. Stoffels, J. J. Pérez-Ríos, and S. Schlemmer, J. Mol. Spectrosc. **332**, 67 (2017).
[30] A. Stoffels, L. Kluge, S. Schlemmer, and S. Brünken, Astron. Astrophys. **593**, A56 (2016).
[31] S. Lee, D. Hauser, O. Lakhmanskaya, S. Spieler, E. S. Endres, K. Geistlinger, S. S. Kumar, and R. Wester, Phys. Rev. A **93**, 032513 (2016).
[32] S. Chandra, W. H. Kegel, and D. A. Varshalovich, Astron. Astrophys. Suppl. Ser. **55**, 51 (1984), http://adsabs.harvard.edu/full/1984A%26AS...55...51C.
[33] M. A. Martin-Drumel, O. Pirali, and M. Vervloet, J. Phys. Chem. A **118**, 1331 (2014).
[34] J. M. Cook, G. W. Hills, and R. F. Curl, J. Chem. Phys. **67**, 1450 (1977).
[35] D. Gerlich, Phys. Scr. **T59**, 256 (1995).
[36] R. Wester, J. Phys. B **42**, 154001 (2009).
[37] R. Otto, A. von Zastrow, T. Best, and R. Wester, Phys. Chem. Chem. Phys. **15**, 612 (2013).
[38] H. Kreckel, D. Bing, S. Reinhardt, A. Petrignani, M. Berg, and A. Wolf, J. Chem. Phys. **129**, 164312 (2008).
[39] E. S. Endres, G. Egger, S. Lee, O. Lakhmanskaya, M. Simpson, and R. Wester, J. Mol. Spectrosc. **332**, 134 (2017).
[40] S. P. Belov, M. I. Tret'iakov, and R. D. Suenram, Astrophys. J. **393**, 848 (1992).
[41] O. Lakhmanskaya *et al.*, J. Chem. Phys. (to be published).
[42] R. Otto, J. Mikosch, S. Trippel, M. Weidemüller, and R. Wester, Phys. Rev. Lett. **101**, 063201 (2008).